HHS Public Access

Author manuscript

Mitochondrion. Author manuscript; available in PMC 2017 September 01.

Published in final edited form as:

Mitochondrion. 2016 September ; 30: 177–186. doi:10.1016/j.mito.2016.08.002.

Identification of small molecules that improve ATP synthesis defects conferred by Leber's hereditary optic neuropathy mutations

Sandipan Datta, **Alexey Tomilov**, and **Gino Cortopassi**

Dept. of Molecular Biosciences, School of Veterinary Medicine, University of California, Davis, 1089 Veterinary medicine Drive, Davis, CA 95616

Abstract

Inherited mitochondrial complex I mutations cause blinding Leber's hereditary Optic Neuropathy (LHON), for which no curative therapy exists. A specific biochemical consequence of LHON mutations in the presence of trace rotenone was observed: deficient complex I-dependent ATP synthesis (CIDAS) and mitochondrial O_2 consumption, proportional to the clinical severity of the three primary LHON mutations. We optimized a high-throughput assay of CIDAS to screen 1600 drugs to 2, papaverine and zolpidem, which protected CIDAS in LHON cells concentration-dependently. TSPO and cAMP were investigated as protective mechanisms, but a conclusive mechanism remains to be elucidated; next steps include testing in animal models.

Keywords

LHON; mitochondria; high-throughput screening; complex I

1. Introduction

Leber's Hereditary Optic Neuropathy (LHON) is one of the most common forms of mitochondrial disease, wherein 1 out of 30,000 individuals are affected in Northern Europe alone (Chinnery et al., 2000; Hudson et al., 2007; Mascialino et al., 2012). LHON is initially precipitated by painless and acute unilateral loss of central vision, and it gradually manifests as total bilateral vision loss and blindness. Typical pathologic changes observed in LHON include optic nerve atrophy and demyelination, and thinning of the retinoganglial cell layer is common **(Fraser et al., 2010; Mackey et al., 1996)**. The disease is more common in males than females in a 3:1 ratio, and age of onset is usually between 15 to 30 years of age.

The majority of LHON cases (>90%) have been associated with three primary mtDNA mutations, namely: 11778(G>A) (encoding the ND4 subunit of complex I), 3460(G>A)

Corresponding author: Gino Cortopassi gcortopassi@ucdavis.edu.
sddatta@ucdavis.edu, atomilov@ucdavis.edu

(encoding the ND1 subunit of complex I), and 14484(T>C) (encoding the ND6 subunit of complex I) **(Mackey et al., 1996)**. These mutations are known to compromise mitochondrial complex I-driven ATP synthesis **(Baracca et al., 2005)**. A correlation between the primary mutations and the severity of clinical outcomes has been observed (Oostra et al., 1994; Riordan-Eva et al., 1995; Spruijt et al., 2006). The 11778(G>A) mutation is the most common and severe amongst the three primary LHON-associated mutations. Vision loss from this mutation is almost always irreversible, with less than 5% chance of spontaneous visual improvement. The 3460(G>A) mutation confers intermediate severity with less than 40% chance of recovery. Lastly, the 14484(T>C) mutation is the least severe and corresponds with less than 65% chance of recovery.

There is currently no FDA-approved therapy for LHON, thus there is a great unmet need for the treatment of this disease. One strategy to expedite LHON drug discovery is to repurpose already FDA-approved/clinically trialed drugs for a new indications. We utilized a repurposing approach to screen for 1600 compounds that have already been FDA-approved/clinically established and might rescue the effects of LHON in cell models. We first identified a rotenone-dependent defect in mitochondrial complex I that represented the severity of ATP synthesis defects in three LHON mutant cytoplasmic hybrids (cybrids). Then we converted this assay to a high-throughput, rotenone-dependent *in-vitro* screen and evaluated the efficacy of a library of 1600 clinically tested drugs on rescuing LHON-dependent ATP synthesis defects. Two drugs, papaverine and zolpidem, were identified in this screen to rescue the LHON-dependent defects in ATP synthesis. Papaverine is an opium alkaloid popularly used as a vasodilator and in erectile dysfunction, while zolpidem, a synthetic imidazopyridine molecule is prescribed clinically as a sleep aid. According to the preliminary data, both papaverine and zolpidem may require the mitochondrial translocator protein (TSPO) and/or PKA activity to exert their rescue effects on the rotenone-dependent mitochondrial complex I defect in LHON mutant cybrids. These relatively safe molecules could be considered as new drug leads for LHON therapy.

2. Materials and methods

2.1 Cell lines and cell culture

The osteosarcoma cytoplasmic hydrids (cybrids) was a kind gift from Drs. Valerio Carelli and Andrea Martinuzzi. These cybrids were originally constructed by fusing 143B 206 rho-zero cell line with enucleated fibroblasts from patients that contained no disease-related mtDNA mutations and LHON patients harboring the 11778(G>A), 3460(G>A), and 14484(T>C) pathogenic mtDNA mutations **(King and Attardi, 1989)**. The resulting cells underwent selection by growth in uridine-free medium supplemented with bromodeoxyuridine. The presence of the LHON pathogenic mutations were then confirmed in the resulting clones **(Torroni et al., 1997)**. The osteosarcoma cybrid cells were cultured in Dulbecco's Modified Eagle's Medium (DMEM) containing 2 mM L-glutamine and 100 mM sodium pyruvate, under 5% carbon dioxide at 37 °C. The medium was further supplemented with 10% fetal bovine serum, 50 μg/mL uridine and antibiotics (50 units/mL of penicillin/50 μg/mL of streptomycin).

The control (Cat# GM13068) and the LHON 11778(G>A) mutant (Cat# GM10742) lymphoblast cells were obtained from Coriell Cell repositories. The lymphoblast cells were cultured in RPMI 1640 medium (Corning) supplemented with 15% FBS, 2 mM L-glutamine, and antibiotics (50 units/mL of penicillin/ 50 μg/mL of streptomycin). The lymphoblasts were cultured under 5% carbon dioxide at 37 °C.

2.2 Chemicals

The Pharmakon collection containing 1600 FDA-approved/clinically evaluated drugs (10 mM, DMSO) was purchased from Microsource Discovery Systems Inc. Papaverine (#P3510), zolpidem (#Z103), PK11195 (#C0424), streptolysin O (#S5265), and rotenone (#R8875) were purchased from Sigma-Aldrich. The PKA inhibitor H89 (#2910) and $GABA_A$ antagonist bicuculline (#0130) was obtained from Tocris. The ATP bioluminescence kit CLSII was obtained from Roche. The ATP-free ADP was obtained from Appollo scientific and Cell technology. All the other chemicals and reagents were obtained from Sigma-aldrich unless otherwise specified.

2.3 Measurement of complex I-driven ATP synthesis (CIDAS)

The cybrid cells was seeded at 50,000 cells/well in 100 μL of culture medium, in a white, opaque-bottom, 96-well plate coated with poly-D-Lysine (Corning) and was incubated at 37 °C overnight. The drugs were dissolved in serum-free medium and 100 μL of 2x drug solution was added to the cells. After the drug-treated cells were incubated for 22 h at 37 °C, 100 μL of conditioned medium was removed from the wells and 100 μL of medium containing rotenone (2x) was added to the cells. After 2 h incubation at 37 °C, the medium from the plates was aspirated using an automatic plate washer (Biotek) and complex I-driven ATP synthesis was measured following the protocol of Yoshida and Fujikawa **(Fujikawa and Yoshida, 2010)** modified by us. Briefly, after aspirating the conditioned medium, the drug and rotenone-treated cells was permeabilized using streptolysin O (SLO). The plasma membrane permeabilization was done in two steps. First SLO was allowed to attach the plasma membrane at 0 °C. Then the extra SLO was removed and subsequently the attached SLO was activated at 37 °C for permeabilization. Plate washes was minimized in order to prevent the cell loss. The permeabilized cells was incubated for 20 min with high purity ATP-free ADP (200 μM, Apollo Scientific) and complex I substrates, Malate (5 mM) and Pyruvate (5 mM). The steady state ATP concentration in each well was measured by using ATP Bioluminescence Assay Kit CLS II (Roche) following manufacturer's instructions. The ATP synthesis rate was calculated by ATP conc. (μM) in each well/Incubation time (20 min). The entire assay was done in a HTS system (96-well format) and all analyses were performed under confluent conditions.

For the lymphoblasts, drug-treated cells were centrifuged and resuspended at a concentration of 2×10^6 cells/mL in the permeabilization buffer containing activated streptolysin O (Sigma). After 10 min incubation at 4 °C, the cells were centrifuged and resuspended in transfer buffer at the same concentration. The cells were then incubated at 37 °C for 10 min followed by centrifugation and resuspension in buffer A **(Fujikawa and Yoshida, 2010)** supplemented with complex I substrates malate (5 mM, Sigma), sodium pyruvate (5 mM, Sigma) and high purity ATP-free ADP (200 μM, Apollo Scientific). Subsequently, 50 μL of

buffer A containing 100,000 cells were plated in each wells of a 96-well plate. After 20 min of incubation at the room temperature the steady state ATP concentration in each well was measured by using ATP Bioluminescence Assay Kit CLS II (Roche) following manufacturer's instruction. The ATP synthesis rate was calculated by ATP conc. (μM) in each well/Incubation time (20 min).

2.4 Drug screening and hits identification

The 1600 drugs were screened using the CIDAS assay described above. The test compounds (10 mM, DMSO) were diluted to 20 μM with serum-free culture medium and 100 μL of the diluted solutions were added to the cells. Vehicle treated cells (4 wells) were used as a positive control and rotenone (0.1 μM) treated cells (4 wells) were used as negative controls. Each drug was assayed in duplicate.

Fold change of ATP synthesis rate over the plate median for each drug-treated well was calculated. The drugs showing a fold change greater than 2x median absolute deviation (MAD) were considered as preliminary hit. The preliminary hits were further assayed for their protective activity in the CIDAS assay using a 6-point concentration response curve in triplicate. The drugs that showed a concentration-dependent protective effect were confirmed as a hit. The hits were then prioritized by the magnitude of their protective effect shown in the concentration response curve.

2.5 Oxygen consumption measurements using a Seahorse XF-24 system

Control and mutant LHON cybrids cells were seeded at a density of 50000 cells/well in 200 μL of culture medium, in a 24-well seahorse tissue culture plate (Seahorse Biosciences, Billerica, MA, USA), and was incubated overnight. Before the measurement medium was changed to unbuffered DMEM, 20% FBS, 200 mM glutamax, 100 mM sodium pyruvate, 25 mM glucose, pH 7.4 without phenol red. Cells were pre-equilibrated for 20 min. The oxygen consumption rate (OCR) was recorded using a Seahorse XF-24 instrument and measured oxygen consumption per minute in pmol (pmol/min). The OCR was measured before (basal) and after addition of rotenone at the specified concentrations. Percentage of the basal OCR was calculated using the formula:

$$\% \text{ Basal OCR} = \text{OCR after addition of rotenone} / \text{OCR before addition of rotenone}$$

2.6 qPCR for determination of mtDNA/nDNA ratio

Control and LHON mutant cybrid cells were treated with vehicle or the drugs at the specified concentration for 24 h. Subsequently, total cellular DNA was extracted using DNeasy plus mini kit (Qiagen, Valencia, CA, USA) respectively following manufacturer's instruction. Isolated DNA was quantified by NanoDrop 2000c Spectrophotometer (Thermo Scientific, Waltham, MA, USA).

Human MT-TL1 and human β-2-microglobulin was selected as the representative mitochondrial and nuclear gene respectively. The Species Gene Sequence (5' → 3') was Human MT-TL1 (DNA) Forward CACCCAAGAACAGGGTTTGT MT-TL1 (DNA) Reverse TGGCCATGGGTATGTTGTTA Human B2M (DNA) Forward

TGCTGTCTCCATGTTTGATGTATCT B2M (DNA) Reverse TCTCTGCTCCCCACCTCTAAGT. The qPCR on the isolated DNA was performed using the SensiFAST SYBR No-ROX Kit (Bioline, Taunton, MA, USA) in a Roche Lightcycler 480 (Roche Diagnostics, Indianapolis, IN, USA). Second derivative of the amplification curve was used to determine the cycle threshold and the data were analyzed by delta delta CT calculation.

2.7 Data analysis

Data are presented as mean ± standard deviation (SD). The data was analyzed using one-way or two-way ANOVA followed by Bonferonni's or Dunett's post hoc analysis, wherever applicable. The *P*-value < 0.05 was considered as statistically significant. Statistical data analysis and curve fitting was performed in Graphpad prism 5.0 using nonlinear regression analysis with variable slope.

3. Results & discussion

3.1 Optimizing a high-throughput assay to quantify mitochondrial complex I-driven ATP synthesis

Previous reports indicate that LHON mutations in mtDNA lead to defect(s) in complex-I-driven ATP synthesis **(Baracca et al., 2005)**. Using an existing high-throughput screening (HTS) assay **(Fujikawa and Yoshida, 2010)** we observed a Z' of below 0.4, which was insufficient criterion for HTS. Therefore, we tested multiple parameters and ultimately found that decreasing the number of plate washes from 6 to 2 was absolutely essential to reduce inconsistent cell loss across the plate and therefore, output variability. The reduction in plate wash and using optimal cybrid cell density of 50,000 cells/well ultimately resulted in a Z'= >0.4. We additionally utilized different substrates and inhibitors of mitochondrial complexes to confirm that the luminescence observed in the assay was specifically from mitochondrial ATP synthesis. As expected, rotenone (1 μM), Antimycin (1 μM), and Oligomycin (1 μM) inhibited mitochondrial ATP synthesis. Succinate (5 mM) and Ascorbate/TMPD reversed the rotenone and antimycin inhibition, respectively (Fig. S1-Supplementary material).

3.2 LHON mutations sensitize complex I to rotenone.

Among the various LHON-associated mutations, the 11778(G>A) mutation encoding the ND4 subunit of mitochondrial complex I is the most prevalent and the most severe **(Oostra et al., 1994)**. Rotenone is a complex I inhibitor that binds in the ND4 subunit **(Degli Esposti et al., 1994)**. We tested the rotenone-sensitivity of LHON cybrids vs. control cybrids and found their CIDAS to be more sensitive, supporting the idea that the decreased CIDAS is conferred by the 11778 mutation and not the cell type (Fig. 1A). Two different clones of LHON mutant cybrid cells (HCT22 and HFF3) and control cybrid cells (HGA2 and H1959) were treated with rotenone (0.001 μM – 1 μM) in half-log increments, and CIDAS was measured after 24 h. The CIDAS in 11778(G>A) mutant cybrids was decreased to ~20% of control in the presence of rotenone (0.1 μM), presenting an adequate screening window (Fig. 1A). The rotenone treatment (24 h), however, did not affect the cell viability of the cybrids (data not shown). Thus, rotenone uncovers a LHON-specific biochemical sensitivity of approximately 3-fold greater sensitivity than controls.

To determine whether the rotenone-dependent CIDAS sensitivity was the result of LHON mutation or some property of the osteosarcoma cell type, rotenone-dependent CIDAS was measured in lymphoblasts derived from LHON patients and controls. The differential effect of rotenone on the 11778(G>A) mutant was clearly reproducible in the lymphoblast cell lines from human LHON patients (Fig. 1B). Thus, rotenone-sensitivity is a consistent consequence of LHON mutations across cell types.

3.3 HON mutation sensitizes the mitochondrial O_2 consumption to rotenone

Mitochondrial O_2 consumption is an indirect measure of the mitochondrial electron transport chain activity. Just as LHON cells' CIDAS were more sensitive to rotenone, so was the LHON cells' ability to carry out mitochondrial O_2 consumption (Fig. 2A.). Similar to the effects on CIDAS, 11778(G>A) mutant cells were four times more sensitive to rotenone (IC_{50} 4.7 nM) compared to control cells (IC_{50} 21.3 nM) (Fig. 2A.).

3.4 LHON mutations affect rotenone-sensitive complex I-driven ATP synthesis defect in a manner proportional to mutant severity

We next examined the effects of rotenone on the other two most common LHON mutations in cybrids to determine if the screening parameters were identifying a biochemical difference that was conferred by the severity of LHON mutations. Interestingly, the effect of the biochemical defect in ATP synthesis was directly in proportion to the severity of the disease in humans. That is, the 11778(G>A) mutation had the most severe ATP defect, G3460A had an intermediate effect, and T14484C showed the mildest effect (Fig. 2B). The degree that each cybrid LHON mutant model affects rotenone-dependent CIDAS is similar to the degree of disease severity in respective human LHON mutations (Fig. 2B). This suggests the CIDAS defect is both a biochemical measure of disease severity and also of drug effect.

3.5 Screening a library of clinically-used drugs with known pharmacokinetic and safety profiles for rescue of LHON-dependent rotenone sensitivity

In order to identify drug leads for LHON, rotenone-inhibited CIDAS was used as an assay to find potential drug therapies for this disease. We hypothesized that the LHON genetic mutations confer a rotenone-dependent CIDAS defect, and that rescue of this deficient CIDAS could be used to identify potential LHON therapeutics. Since the 11778(G>A) mutation is the most prevalent LHON-associated mutation and showed the highest rotenone-dependent ATP synthesis inhibition compared to the other LHON mutants, the HCT22 11778(G>A) clone was used for further drug screening.

We screened the Pharmakon™ collection (Microsource Discovery Systems) of 1,600 FDA-approved and/or clinically evaluated drugs in duplicate, in a 96-well format. Drugs that consistently showed an enhancement of ATP synthesis rate greater than two times of the Median absolute deviation (MAD) in both plates were considered preliminary hits. The preliminary hits were subject to the same assay in triplicate for reconfirmation. The analysis initially identified 34 preliminary hits; however, only 2/34 drugs were confirmed in six-point dose curves from 0.1 μM to 30μM at half-log increments. Based on their magnitude of rescue effects, the top hit was identified as papaverine, a phosphodiesterase inhibitor, and the

other hit was Zolpidem, an agonist of γ-aminobutyric acid receptor subtype A ($GABA_A$), and peripheral benzodiazepine receptor PBR, also known as TSPO (Fig. 3A-B).

3.6 Papaverine and zolpidem concentration-dependently protect CIDAS

Papaverine, an isoquinoline opium alkaloid, was the more active and potent drug to increase CIDAS in the preliminary screen, at a single concentration (10 μM). When characterized further, papaverine concentration-dependently reversed rotenone sensitivity in LHON 11778(G>A) mutant cells (Fig. 4A). In addition, we determined its specificity for LHON and control cells (Fig. 4C). When CIDAS was inhibited to about 30% of basal in both control and LHON cells, papaverine clearly increased CIDAS more in LHON cells than controls. The effect of papaverine was about 3-4 fold in LHON cells vs 2-fold in CTL cells. Thus papaverine has a greater rescue effect on LHON cells than controls. However, it also has measurable activity in CTL cells inhibited with rotenone.

Since the inhibition of ATP synthesis by 0.1 μM rotenone was approximately 90%, we were concerned that it might be insensitive to the lower concentrations of papaverine. In order to detect the accurate concentration response curves, we lowered the concentration of rotenone to 0.03 μM for concentration response studies. This concentration was the lowest concentration of rotenone which confers significant difference in CIDAS sensitivity.

The $GABA_A$ receptor-agonist zolpidem also concentration-dependently reversed the rotenone sensitivity of both the CTL and 11778(G>A) LHON cybrid cells, although to a lesser extent than papaverine (Fig. 4B). Mutant cells pre-treated with zolpidem (3, 10, and 30 μM) showed a significantly higher ATP synthesis rate when subsequently treated with 0.03 μM rotenone compared to pre-treated vehicle cells. The ATP synthesis rate in the 30 μM zolpidem-treated LHON mutant cells was increased 2 folds than the vehicle-treated cells after rotenone treatment (0.03 μM) (Fig. 4B).

3.7 Papaverine rescues complex I defects specifically

Papaverine and Zolpidem might theoretically be working generally, to increase mitochondrial function overall, or might be working specifically at complex I. We investigated papaverine and zolpidem specificity, with inhibitors that act at different mitochondrial sites: rotenone, Antimycin A, Oligomycin and FCCP (Fig. 5A-D). If papaverine was boosting mitochondrial function generally or was a mitoproliferative drug, we would expect it to reverse the mitochondrial inhibition globally, whichever inhibitor was used--we did not observe this. By contrast with this global hypothesis, what we observed was that papaverine reversed only rotenone-dependent decrease in ATP synthesis in a concentration-dependent manner.

A separate test of specificity is to feed complex II substrates and test the effects of papaverine, if papaverine increases mitofunction globally it should increase the complex II dependent synthesis of ATP--but we did not observe this. What we observed was no effect of papaverine on the ATP synthesis rate driven by the complex II substrate succinate (Fig. 5E).

3.8 olpidem rescues complex I defect specifically

Zolpidem, like papaverine, did not rescue the effects of other inhibitors in a concentration-dependent manner, outside of complex I. (Fig 6A-D). These data suggest that similar to papaverine, the enhancement of CIDAS in the presence of rotenone by zolpidem is complex I-specific.

3.9 Papaverine and Zolpidem rescues submaximal LHON-dependent inhibition of CIDAS in the presence of rotenone

Papaverine and Zolpidem were identified through their ability to rescue a submaximal level of CIDAS limited by LHON mutations plus trace rotenone. Given that they rescue of submaximal ATP synthesis, specifically overcoming a complex I, we asked the broader question of whether Papaverine and Zolpidem could boost CIDAS even when there was not a LHON or rotenone-dependent defect. We did not observe a boosting of CIDAS in non-LHON or non-rotenone treated cells (Fig. S2-Supplementary material)

3.10 Testing the mechanism of rescue of submaximal CIDAS in cells and permeabilized cells

Both papaverine and zolpidem concentration-dependently reverse the effects of submaximal complex I activity in rotenone-inhibited LHON cells, and their effect is specific to complex I. One possible explanation for this protection is that papaverine or zolpidem directly competes with rotenone's binding site on complex I. One test of this hypothesis is to carry out the test of protection in cells and permeabilized cells. If either papaverine or zolpidem is a rotenone displacer, then their displacement activity should occur both in whole live cells or permeabilized cells. We observed that contrary to the expectation for a rotenone displacer, Papaverine did not protect from rotenone inhibition in the context of permeabilized cells, although it clearly did in cells (Fig. 7A). Thus papaverine does not displace rotenone on complex I, and it appears likely that papaverine's target is extramitochondrial, because direct access to mitochondria in permeabilized cells disrupts its protective effect.

Zolpidem's major protective effect on CIDAS was observed in cells (Fig.7B), also supporting an extramitochondrial target. However, a small amount of Zolpidem-mediated protection was observed in permeabilized cells (38%), suggesting that Zolpidem could also act at a mitochondrial site, either displacing rotenone from mitochondria or limiting rotenone's access to mitochondria.

3.11 Papaverine and Zolpidem do not increase mitochondrial biogenesis

Another possible mechanism for reversal of rotenone sensitivity is enhancement of global mitochondrial biogenesis. A concentration-dependent increase in mitochondrial population can result in increased ATP synthesis. Hence, we evaluated the effects of the drugs on mitochondrial copy number. Neither papaverine nor Zolpidem significantly altered mtDNA/nDNA ratio in LHON or control cells after 24h of exposure, thus rescue does not appear to be the result of a mitoproliferative effect of the drugs (Figs. 8A-B).

3.12 Study of papaverine and zolpidem's nominal mechanism and relationship to mitochondrial mechanism

Both Papaverine and Zolpidem have nominal targets, phosphodiesterase 10 and $GABA_A$ receptor, and so the relationship of the mitochondrial CIDAS effects to known targets were studied by known phosphodiesterase and GABA modulators. Papaverine's nominal target is considered to be the inhibition of phosphodiesterase 10 (PDE10) **(Chappie et al., 2007)**. Phosphodiesterases degrade cyclic AMP (cAMP), in a desensitization response **(Bender and Beavo, 2006; Moorthy et al., 2011)**. Papaverine is a known inhibitor of cAMP/cGMP phosphodiesterases and is known to increase cellular cAMP levels **(Torremans et al., 2010)**. This was interesting because the extramitochondrial cAMP-PKA signaling axis has been postulated to increase mitochondrial function and biogenesis, i.e. ligand->cAMP->PKA->mitochondrial stimulation **(Feliciello et al., 2005)** . Recent studies have also determined that intramitochondrial cAMP regulates mitochondrial PKA and is a major regulator of oxidative phosphorylation **(Acin-Perez et al., 2009; Valsecchi et al., 2013).** We thus tested the hypothesis that papaverine's protective effect is mediated through its phosphodiesterase inhibitory- and protein kinase A-stimulatory effect, which is known to stimulate mitochondrial functions. The PKA inhibitor H89 (Gomez-Concha et al., 2011; Valsecchi et al., 2013) and the protein kinase A stimulator forskolin **(Li et al., 2008)** were used to test whether papaverine’s mechanism of action involved cAMP-protein kinase A. Forskolin, a potent stimulator of cellular cAMP production, would be predicted to reproduce the stimulatory effect of papaverine if papaverine were working through a cAMP mechanism. Forskolin administration at physiologically relevant doses also did not produce any measurable protection of CIDAS (data not shown). Similarly, we observed no suppression of papaverine's ability to boost CIDAS in the context of the PKA inhibitor H89 (Fig. S3-Supplementary Material). Thus, our data do not support the idea that papaverine's protective effect is mediated through stimulation of the cAMP-PKA signaling pathway.

3.13 Assessing the possible cytoplasmic mechanism of zolpidem

Zolpidem's major activity is in whole cells, and there is only a small protection that could be attributed to rotenone displacement at complex I. Zolpidem is known to be a $GABA_A$ receptor agonist **(Crestani et al., 2000)**; thus, the effect of zolpidem on LHON mutant cells might be $GABA_A$-mediated. However the $GABA_A$ antagonist bicuculine had no significant effect on the concentration-dependent reversal of rotenone inhibition by zolpidem in 11778(G>A) cybrid cells (Fig. S4-Supplementary Material).

The possible involvement of the cAMP-PKA signaling axis in zolpidem’s mechanism of action was also evaluated using the PKA inhibitor H89. Incubation of H89 (3 μM) with zolpidem (30 μM) reversed the rotenone rescue effect of zolpidem (Fig. 9). However, the concentration of H89 required to completely reverse the protective effect of zolpidem is much higher than its PKA inhibitory concentrations (IC_{50} 135 nM). Thus, it is likely that the protective effect of zolpidem is mediated through some other kinases for which further investigation is necessary.

3.14 Papaverine and zolpidem combination show additive effect

Since papaverine and zolpidem appear to have different mechanisms based on inhibitor-suppression and different effects in whole-vs permeabilized cells, we tested whether the combination of these two drugs would be more effective than either of these drugs alone. Indeed when combined together the protection from rotenone inhibition by the combination was much higher than that of either papaverine (10 μM) or zolpidem (30 μM) alone (Fig. 10). These two concentrations were selected for combination study because they provided the highest response.

3.14 Could TSPO be a common mechanism for both papaverine and zolpidem?

Another possible hypothesis was that zolpidem might be acting through the mitochondrially-localized TranSlocator PrOtein (TSPO), also known as the peripheral benzodiazepine receptor. The TSPO antagonist PK11195 effectively blocked the stimulatory action of papaverine and zolpidem (Fig. 11A-B). The inhibition of papaverine and zolpidem's CIDAS-stimulating activity by PK11195 can be dose-dependently overcome by papaverine (30 μM) and zolpidem (50 μM), suggesting a competitive antagonism by PK11195. This suggests that the role of TSPO in the mitochondrial protection needs further investigation.

4. Summary and conclusions

Evidence-based drug discovery for LHON is urgently needed, as no effective LHON drug currently exists. In this study we demonstrated that LHON mutant cells have a mutation-specific sensitivity in the CIDAS parameter that is uncovered by rotenone, and this parameter is proportional to the disease-severity of the mutation. We used this LHON-dependent sensitivity and an improved HTS assay of CIDAS to screen 1600 small molecules that have passed through clinical testing. The top two hits, zolpidem and papaverine, were reconfirmed and showed a concentration-dependent, complex I-specific, submaximal CIDAS-stimulating response. The mechanisms of these drugs are not completely clear but the data suggests that one of them might exert their effects through rotenone displacement and/or the cAMP-PKA axis. Further experiments are needed to elucidate the complete *in vitro* mechanism of action of these small molecules and their *in vivo* efficacy in a LHON animal model.

Supplementary Material

Refer to Web version on PubMed Central for supplementary material.

Acknowledgement

This work was supported by the following awards: EY012245, NS077777.

We would also like to thank Sunil Sahdeo and Jennifer Gray for their inputs in experimental design and editing respectively.

References

Acin-Perez R, Salazar E, Kamenetsky M, Buck J, Levin LR, Manfredi G. Cyclic AMP produced inside mitochondria regulates oxidative phosphorylation. Cell metabolism. 2009; 9:265–276. [PubMed: 19254571]

Baracca A, Solaini G, Sgarbi G, Lenaz G, Baruzzi A, Schapira AH, Martinuzzi A, Carelli V. Severe impairment of complex I-driven adenosine triphosphate synthesis in leber hereditary optic neuropathy cybrids. Archives of neurology. 2005; 62:730–736. [PubMed: 15883259]

Bender AT, Beavo JA. Cyclic nucleotide phosphodiesterases: molecular regulation to clinical use. Pharmacological reviews. 2006; 58:488–520. [PubMed: 16968949]

Chappie TA, Humphrey JM, Allen MP, Estep KG, Fox CB, Lebel LA, Liras S, Marr ES, Menniti FS, Pandit J, Schmidt CJ, Tu M, Williams RD, Yang FV. Discovery of a series of 6,7-dimethoxy-4-pyrrolidylquinazoline PDE10A inhibitors. Journal of medicinal chemistry. 2007; 50:182–185. [PubMed: 17228859]

Chinnery PF, Johnson MA, Wardell TM, Singh-Kler R, Hayes C, Brown DT, Taylor RW, Bindoff LA, Turnbull DM. The epidemiology of pathogenic mitochondrial DNA mutations. Annals of neurology. 2000; 48:188–193. [PubMed: 10939569]

Crestani F, Martin JR, Mohler H, Rudolph U. Mechanism of action of the hypnotic zolpidem in vivo. British journal of pharmacology. 2000; 131:1251–1254. [PubMed: 11090095]

Degli Esposti M, Carelli V, Ghelli A, Ratta M, Crimi M, Sangiorgi S, Montagna P, Lenaz G, Lugaresi E, Cortelli P. Functional alterations of the mitochondrially encoded ND4 subunit associated with Leber's hereditary optic neuropathy. FEBS letters. 1994; 352:375–379. [PubMed: 7926004]

Feliciello A, Gottesman ME, Avvedimento EV. cAMP-PKA signaling to the mitochondria: protein scaffolds, mRNA and phosphatases. Cellular signalling. 2005; 17:279–287. [PubMed: 15567059]

Fraser JA, Biousse V, Newman NJ. The neuro-ophthalmology of mitochondrial disease. Survey of ophthalmology. 2010; 55:299–334. [PubMed: 20471050]

Fujikawa M, Yoshida M. A sensitive, simple assay of mitochondrial ATP synthesis of cultured mammalian cells suitable for high-throughput analysis. Biochemical and biophysical research communications. 2010; 401:538–543. [PubMed: 20875793]

Gomez-Concha C, Flores-Herrera O, Olvera-Sanchez S, Espinosa-Garcia MT, Martinez F. Progesterone synthesis by human placental mitochondria is sensitive to PKA inhibition by H89. The international journal of biochemistry & cell biology. 2011; 43:1402–1411. [PubMed: 21689781]

Hudson G, Carelli V, Spruijt L, Gerards M, Mowbray C, Achilli A, Pyle A, Elson J, Howell N, La Morgia C, Valentino ML, Huoponen K, Savontaus ML, Nikoskelainen E, Sadun AA, Salomao SR, Belfort R Jr. Griffiths P, Man PY, de Coo RF, Horvath R, Zeviani M, Smeets HJ, Torroni A, Chinnery PF. Clinical expression of Leber hereditary optic neuropathy is affected by the mitochondrial DNA-haplogroup background. American journal of human genetics. 2007; 81:228–233. [PubMed: 17668373]

King MP, Attardi G. Human cells lacking mtDNA: repopulation with exogenous mitochondria by complementation. Science (New York, N.Y.). 1989; 246:500–503.

Li F, Wang D, Zhou Y, Zhou B, Yang Y, Chen H, Song J. Protein kinase A suppresses the differentiation of 3T3-L1 preadipocytes. Cell research. 2008; 18:311–323. [PubMed: 18195731]

Mackey DA, Oostra RJ, Rosenberg T, Nikoskelainen E, Bronte-Stewart J, Poulton J, Harding AE, Govan G, Bolhuis PA, Norby S. Primary pathogenic mtDNA mutations in multigeneration pedigrees with Leber hereditary optic neuropathy. American journal of human genetics. 1996; 59:481–485. [PubMed: 8755941]

Mascialino B, Leinonen M, Meier T. Meta-analysis of the prevalence of Leber hereditary optic neuropathy mtDNA mutations in Europe. European journal of ophthalmology. 2012; 22:461–465. [PubMed: 21928272]

Mihaylova MM, Shaw RJ. The AMPK signalling pathway coordinates cell growth, autophagy and metabolism. Nat Cell Biol. 2011; 13:1016–1023. [PubMed: 21892142]

Moorthy BS, Gao Y, Anand GS. Phosphodiesterases catalyze hydrolysis of cAMP-bound to regulatory subunit of protein kinase A and mediate signal termination. Molecular & cellular proteomics : MCP 10. 2011 M110.002295.

Oostra RJ, Bolhuis PA, Wijburg FA, Zorn-Ende G, Bleeker-Wagemakers EM. Leber's hereditary optic neuropathy: correlations between mitochondrial genotype and visual outcome. J Med Genet. 1994; 31:280–286. [PubMed: 8071952]

Riordan-Eva P, Sanders MD, Govan GG, Sweeney MG, Da Costa J, Harding AE. The clinical features of Leber's hereditary optic neuropathy defined by the presence of a pathogenic mitochondrial DNA mutation. Brain. 1995; 118:319–337. Pt 2. [PubMed: 7735876]

Sakamoto K, Holman GD. Emerging role for AS160/TBC1D4 and TBC1D1 in the regulation of GLUT4 traffic. Am J Physiol Endocrinol Metab. 2008; 295:E29–37. [PubMed: 18477703]

Spruijt L, Kolbach DN, de Coo RF, Plomp AS, Bauer NJ, Smeets HJ, de Die-Smulders CE. Influence of mutation type on clinical expression of Leber hereditary optic neuropathy. Am J Ophthalmol. 2006; 141:676–682. [PubMed: 16564802]

Torremans A, Ahnaou A, Van Hemelrijck A, Straetemans R, Geys H, Vanhoof G, Meert TF, Drinkenburg WH. Effects of phosphodiesterase 10 inhibition on striatal cyclic AMP and peripheral physiology in rats. Acta neurobiologiae experimentalis. 2010; 70:13–19. [PubMed: 20407482]

Torroni A, Petrozzi M, D'Urbano L, Sellitto D, Zeviani M, Carrara F, Carducci C, Leuzzi V, Carelli V, Barboni P, De Negri A, Scozzari R. Haplotype and phylogenetic analyses suggest that one European-specific mtDNA background plays a role in the expression of Leber hereditary optic neuropathy by increasing the penetrance of the primary mutations 11778 and 14484. American journal of human genetics. 1997; 60:1107–1121. [PubMed: 9150158]

Valsecchi F, Ramos-Espiritu LS, Buck J, Levin LR, Manfredi G. cAMP and mitochondria. Physiology (Bethesda, Md.). 2013; 28:199–209.

Highlights

- LHON primary mutations sensitize ATP synthesis to complex I inhibitor rotenone.
- A high-throughput ATP synthesis-based screen was developed for LHON drug discovery.
- A library of 1600 clinically used drugs was screened for repurposing.
- Papaverine and zolpidem individually can rescue the rotenone sensitivity in LHON mutants.
- The combination of the drugs shows an additive effect on ATP synthesis rescue.

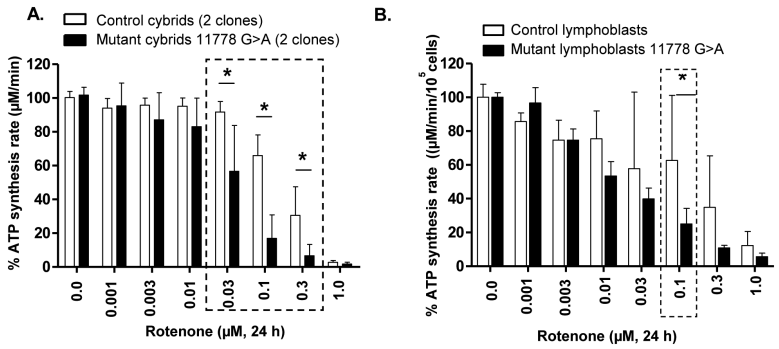

Figure 1.

CIDAS of LHON cybrids and patient lymphoblasts is more sensitive to rotenone than controls. Both LHON cybrids and LHON lymphoblasts are more sensitive to rotenone. (A) Effect of rotenone on control and 11778(G>A) LHON mutant cybrids and (B) effect of rotenone on control and 11778(G>A) mutant lymphoblasts. Cells were treated with different concentrations of rotenone for 24 h and mitochondrial complex I-driven ATP synthesis was measured in permeabilized cells. The data is presented as average + standard deviation from three independent experiments and single asterix signifies the statistical significance ($P < 0.05$) between the control and LHON mutant cells.

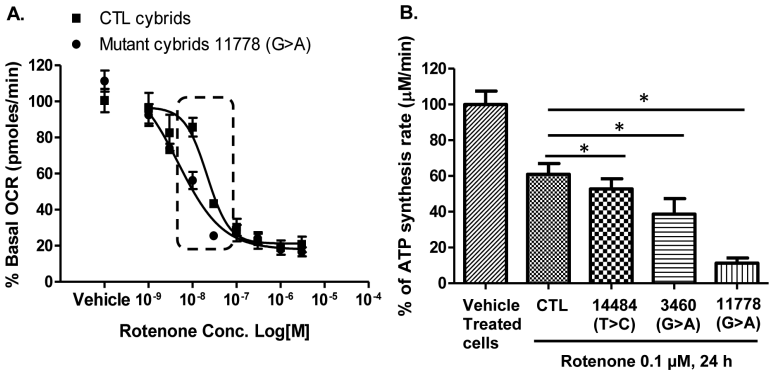

Figure 2.

Effects of rotenone on mitofunctions of CTL and LHON cybrids. (A) Effects of rotenone on mitochondrial O_2 consumption of CTL and 11778 (G>A) mutant cells. Oxygen consumption rate of control and 11778 (G>A) mutant cells was measured 4 times after rotenone addition in a 10 min interval. The data is presented as average percentage of basal/untreated oxygen consumption rate ± standard deviation from three independent experiments. (B) Rotenone sensitivity of ATP synthesis is correlated with severity of disease mutations. Cells with different mutations were treated with rotenone (0.1 µM) for 24 h and mitochondrial complex I-driven ATP synthesis was measured. The data is presented as average + standard deviation from three independent experiments and single asterix signifies the statistical significance ($P < 0.05$) between the control and LHON mutant cells.

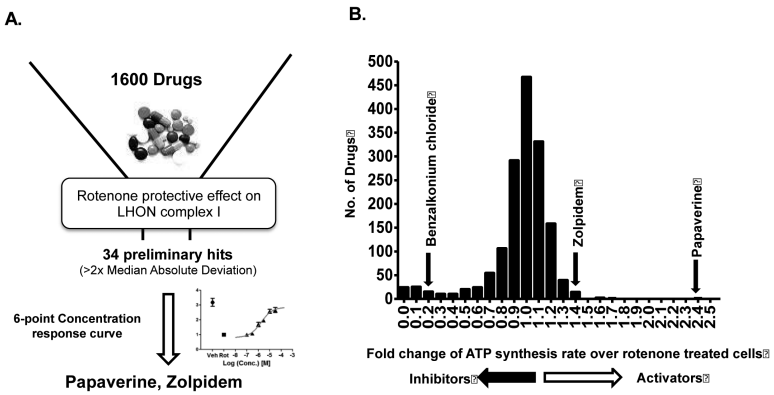

Figure 3.

(A) Schematic representation of the assay workflow; and (B) Histograms of modulators of rotenone-inhibited complex I-driven ATP synthesis in LHON 11778(G>A) cybrids identified by a high-throughput drug screen. The luciferase-based complex I-driven ATP synthesis assay was used to screen a library of 1600 drugs at 10 μM (20 h). The vehicle control was 0.05% DMSO; the negative control was 0.1 μM rotenone. X-axes display mean fold change from plate median in bins of size 0.1 (duplicate). Drugs that increased or decreased luciferase signal than plate median ± two Median absolute deviations were considered preliminary 'hits'. The confirmed activators zolpidem and papaverine are shown above the respective bins corresponding to the response for the drug.

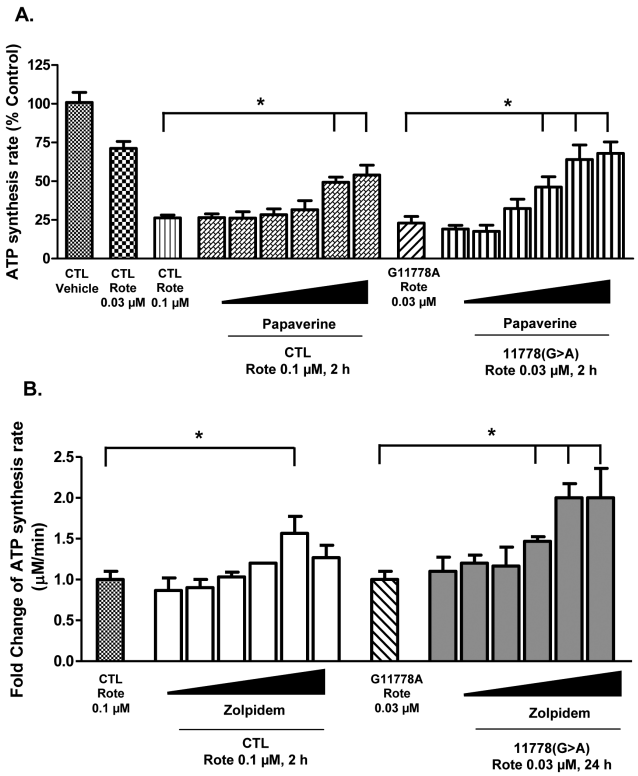

Figure 4.

Concentration-dependent CIDAS-protective effect of (A) papaverine and (B) zolpidem on CTL and LHON mutant [11778(G>A)] cells. Cells were treated with different concentrations of papaverine (0.1, 0.3, 1, 3, 10, and 30 μM) or zolpidem (0.1, 0.3, 1, 3, 10, and 30 μM) for 22 h and subsequently with rotenone (0.03 or 0.1 μM) for 2 h. Cells were permeabilized with streptolysin O and mitochondrial complex I-driven ATP synthesis was measured in presence of complex I substrates (malate/pyruvate). The data is presented as either % control of ATP synthesis rate or fold change over rotenone-treated cells + standard deviation from three independent experiments. Statistical significance ($p < 0.05$) is denoted by "*" and was determined using one-way ANOVA and Dunett's posthoc test in Graphpad Prism 5.0.

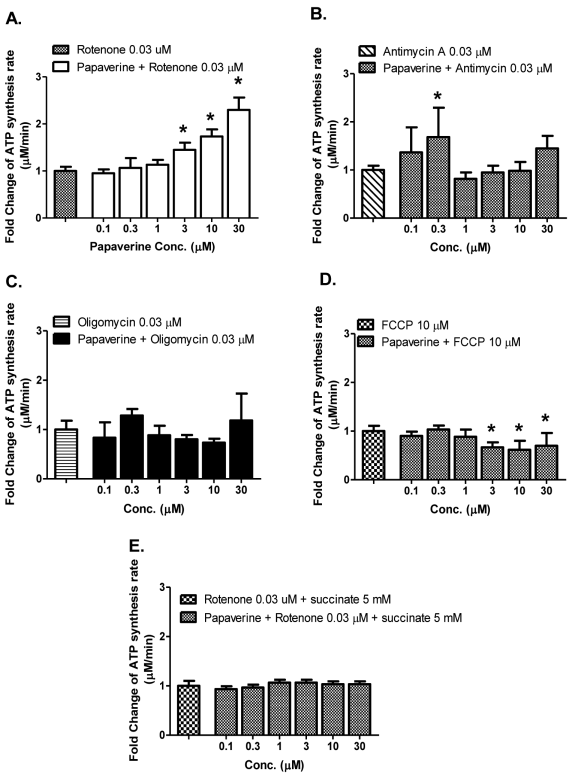

Figure 5.

Complex I specificity of CIDAS-stimulant effect of papaverine, on LHON mutant [11778(G>A)] cybrids. Cells were treated with different concentrations of papaverine for 22 h and subsequently with (A) rotenone (0.03 μM), (B) antimycin A (0.03 μM), (C) oligomycin (0.03 μM), (D) FCCP (10 μM) for 2 h. Cells were permeabilized with streptolysin O and mitochondrial complex I-driven ATP synthesis was measured in presence of complex I substrates (malate/pyruvate) (A-D) or (E) complex II substrate succinate (5 mM). The data is presented as fold change over rotenone/antimycin A/oligomycin/FCCP - treated cells + standard deviation from three independent observations. Statistical significance is denoted by "*" ($p < 0.05$) when compared to respective controls. Statistical significance was determined using one-way ANOVA followed by Dunette's posthoc test in Graphpad Prism 5.0.

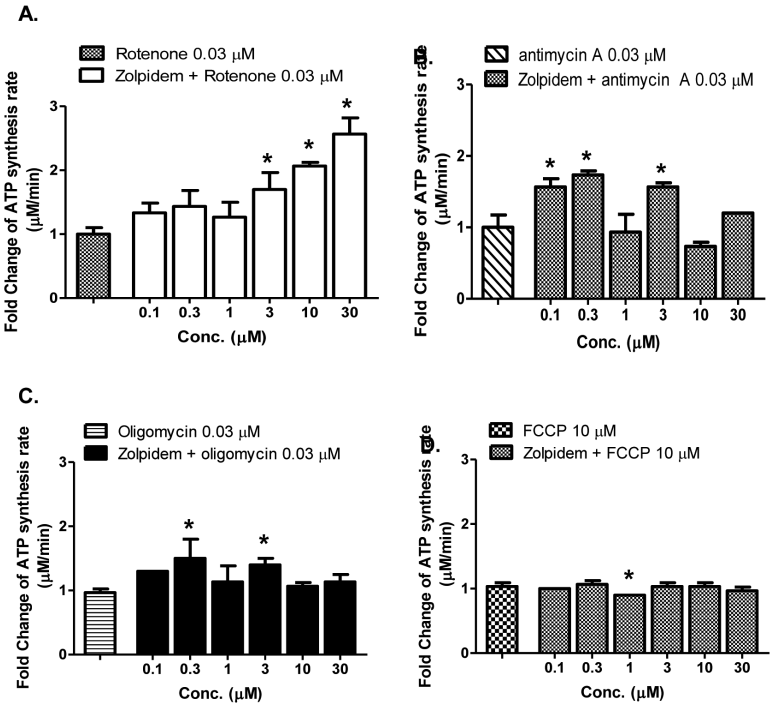

Figure 6.

Complex I specificity of CIDAS-stimulant effect of zolpidem, on LHON mutant [11778(G>A)] cybrids. Cells were treated with different concentrations of zolpidem for 22 h and subsequently with (A) rotenone (0.03 μM); (B) antimycin A; (0.03 μM), (C) oligomycin (0.03 μM); and (D) FCCP (10 μM) for 2 h. Cells were permeabilized with streptolysin O and mitochondrial complex I-driven ATP synthesis was measured in presence of complex I substrates (malate/pyruvate). The data is presented as fold change over rotenone/antimycin A/oligomycin/FCCP-treated cells + standard deviation from three independent observations. Statistical significance is denoted by "*" ($p < 0.05$) when compared to respective controls. Statistical significance was determined using one-way ANOVA followed by Dunette's posthoc test in Graphpad Prism 5.0.

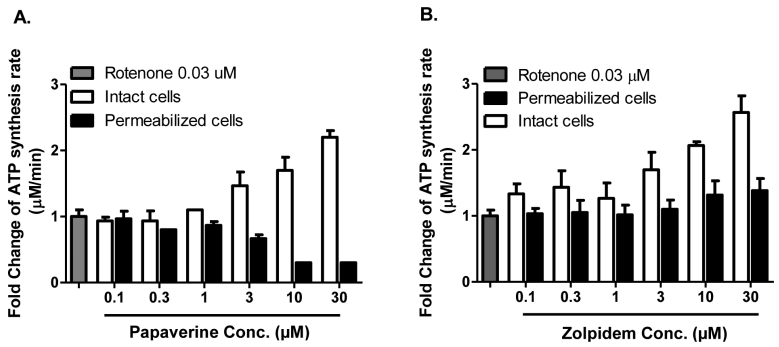

Figure 7.

Effect of (A) papaverine and (B) zolpidem, on rotenone-sensitive CIDAS in intact or permeabilized LHON mutant [11778 (G>A)] cells. Intact cells were treated with different concentrations of papaverine and zolpidem for 22 h and rotenone (0.03 μM) for 2 h. Permeabilized cells were treated with papaverine or zolpidem and rotenone (0.03 μM) for 20 min. Cells were permeabilized with streptolysin O and mitochondrial complex I-driven ATP synthesis was measured in the presence of complex I substrates (malate/pyruvate). The data is presented as fold change over rotenone-treated cells + standard deviation from six independent observations.

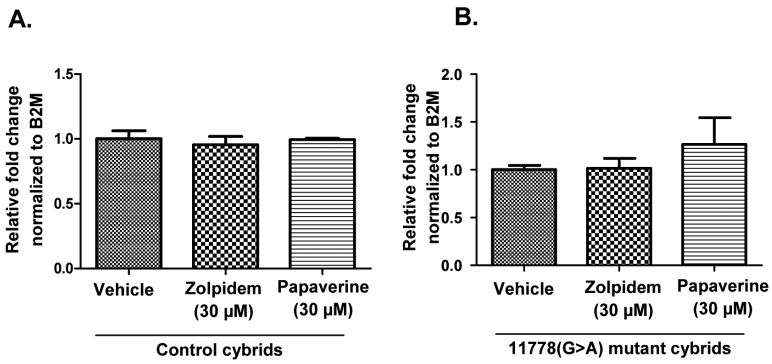

Figure 8.

Effect of zolpidem and papaverine on (A) control cybrid mitochondrial copy number; and (B) 11778(G>A) mutant cybrid mitochondrial copy number. Cells were treated with either vehicle or one of the drugs at specified concentration for 24 h. The cells were harvested after 24 h and the ratio between MT-TL1 and B2M was determined by q-PCR. Data is presented as average relative fold change ± std. deviation from three independent observations. Statistical significance analysis was determined by one way ANOVA and Dunett's post hoc test and no statistical significance was found.

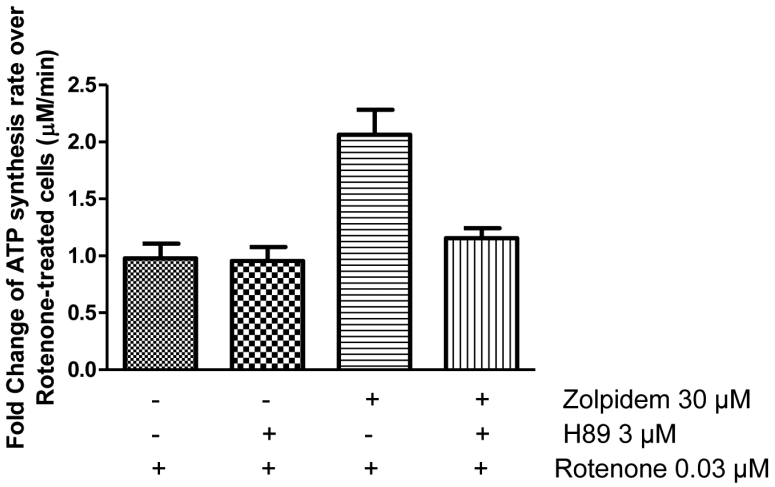

Figure 9.

Reversal of CIDAS-stimulant effect of zolpidem on LHON mutant [11778(G>A)] cells by PKA inhibitor H89. Cells were treated with either vehicle, zolpidem (30 μM) or zolpidem (30 μM) and H89 (3 μM) for 22 h and subsequently with rotenone (0.03 μM) for 2 h. Cells were permeabilized with streptolysin O and mitochondrial complex I-driven ATP synthesis was measured in presence of complex I substrates (malate/pyruvate). The data is presented as fold change over rotenone-treated cells + standard deviation from three independent experiments.

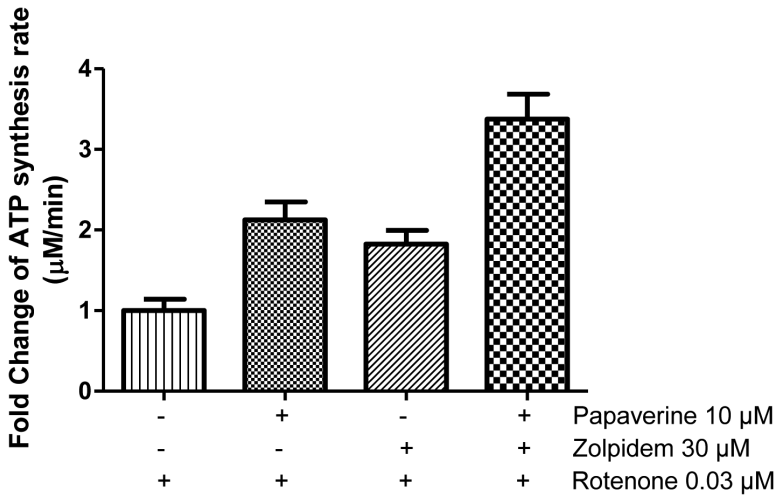

Figure 10.

Additive rotenone de-sensitization effect of papaverine and zolpidem in LHON mutant [11778(G>A)] cells. Cells were treated with either vehicle, papaverine (3 μM), zolpidem (30 μM) or papaverine (3 μM) and zolpidem (30 μM) for 22 h and subsequently treated with rotenone (0.03 μM) for 2 h. Cells were permeabilized with streptolysin O and mitochondrial complex I-driven ATP synthesis was measured in the presence of complex I substrates malate and pyruvate. The data is presented as mean fold change over rotenone-treated cells + standard deviation from four independent observations.

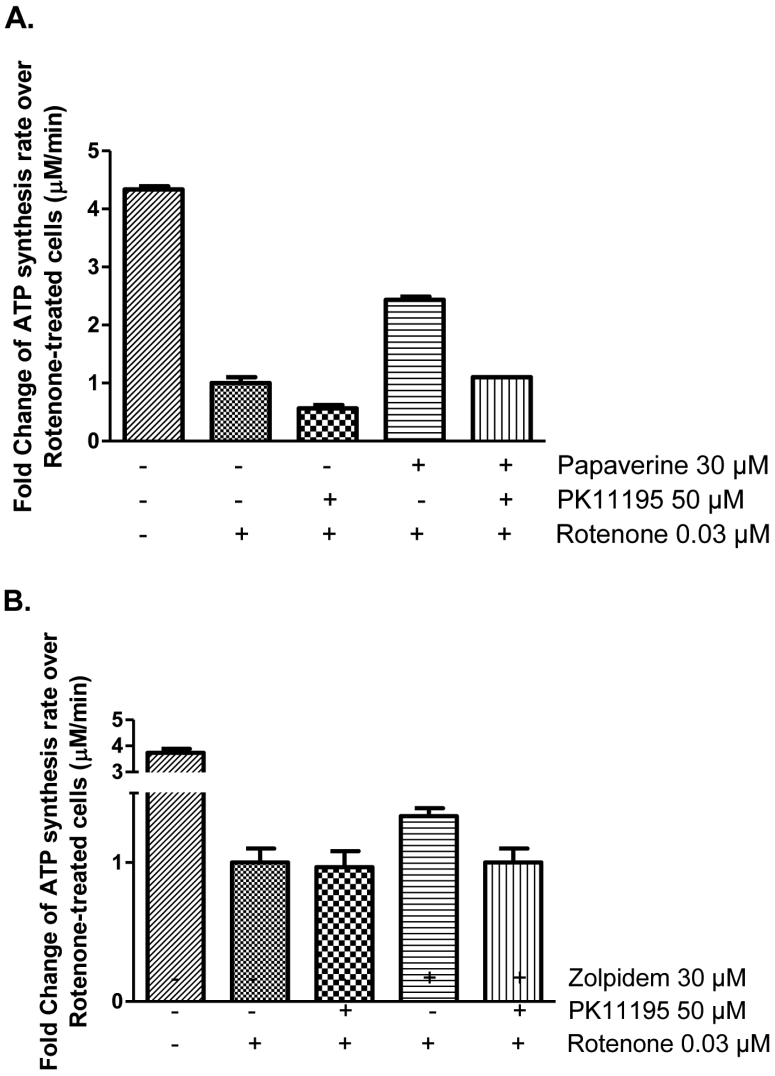

Figure 11.

Reversal of concentration-dependent rotenone de-sensitization effect of papaverine and zolpidem in LHON mutant [11778(G>A)] cells by TSPO antagonist PK11195. (a) Reversal of papaverine rescue effect by PK11195; and (b) Reversal of zolpidem rescue effect by PK11195. Cells were treated with either vehicle, papaverine (10 μM), zolpidem (30 μM) or papaverine (10 μM) and PK11195 (50 μM) or zolpidem (30 μM) and PK11195 (50 μM) for 22 h and subsequently treated with rotenone (0.03 μM) for 2 h. Cells were permeabilized with streptolysin O and mitochondrial complex I-driven ATP synthesis was measured in the presence of complex I substrates malate and pyruvate. The data is presented as fold change over rotenone-treated cells + standard deviation from three independent experiments.